ACS OMEGA

http://pubs.acs.org/journal/acsodf

Article

Using a Mathematical Modeling To Simulate Pharmacokinetics and Urinary Glucose Excretion of Luseogliflozin and Explore the Role of SGLT1/2 in Renal Glucose Reabsorption

Zhongjian Wang,[‖] Guopeng Wang, and Jiawei Ren*

Cite This: *ACS Omega* 2022, 7, 48427−48437

Read Online

ACCESS | Metrics & More | Article Recommendations | Supporting Information

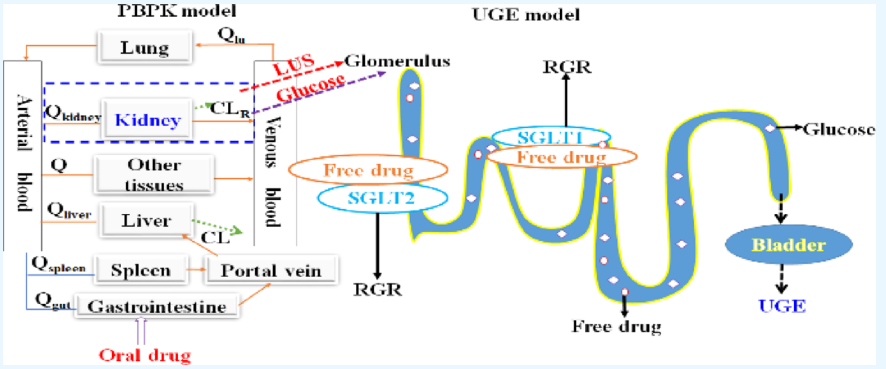

ABSTRACT: (1) Purpose: To develop a mathematical model combining physiologically based pharmacokinetic and urinary glucose excretion (PBPK-UGE) to simultaneously predict pharmacokinetic (PK) and UGE changes of luseogliflozin (LUS) as well as to explore the role of sodium-glucose cotransporters (SGLT1 and SGLT2) in renal glucose reabsorption (RGR) in humans. (2) Methods: The PBPK-UGE model was built using physicochemical and biochemical properties, binding kinetics data, affinity to SGLTs for glucose, and physiological parameters of renal tubules. (3) Results: The simulations using this model clarified that SGLT1/2 contributed 15 and 85%, respectively, to RGR in the absence of LUS. However, in the presence of LUS, the contribution proportion of SGLT1 rose to 52−76% in healthy individuals and 55−83% in T2DM patients, and that of SGLT2 reduced to 24−48 and 17−45%, respectively. Furthermore, this model supported the underlying mechanism that only 23−40% inhibition of the total RGR with 5 mg of LUS is resulted from SGLT1's compensatory effect and the reabsorption activity of unbound SGLT2. (4) Conclusion: This PBPK-UGE model can predict PK and UGE in healthy individuals and T2DM patients and can also analyze the contribution of SGLT1/2 to RGR with and without LUS.

1. INTRODUCTION

The primary kidney transporters that mediate reabsorption of plasma glucose have been identified as two sodium-glucose cotransporters (SGLTs), SGLT1 and SGLT2.[1] In the kidney, SGLT2 resides in the luminal membrane of the early segment (S1) of proximal convoluted segments, and SGLT1 is present in the luminal membrane of the distal segment (S2) of proximal renal tubules.[2,3] Although the quantitative contribution proportion between SGLT1 and SGLT2 to RGR has not been directly determined by experiment in humans yet, there is a general agreement that about 80−90% of renal glucose reabsorption is mediated by SGLT2 and 10−20% by SGLT1.[3,4]

Luseogliflozin (LUS) is an orally administered SGLT2 inhibitor indicated for the treatment of patients with type 2 diabetes (T2DM).[5,6] LUS selectively inhibits SGLT2, which can lead to increased glucose excretion in human urine and, subsequently, reduced blood glucose concentration. LUS was developed by the Taisho company and approved in Japan in 2014.[7] LUS is metabolized by multiple metabolizing enzymes, including cytochrome P450 (CYP), uridine diphosphate glucuronosyltransferase (UGT), alcohol dehydrogenase, and aldehyde dehydrogenase and through multiple pathways like oxidation and glucuronidation.[8] Twenty metabolites were identified in human plasma and urine.[8] Of all metabolites, M2 is the only active one with a half maximal inhibitory concentration (IC_{50}) of 4.01 nM toward SGLT2[9] and the amount of M2 in plasma is the highest but only accounts for approximately 13.5% of unchanged LUS.[10] Additionally,

Received: October 17, 2022
Accepted: December 6, 2022
Published: December 15, 2022

Table 1. Summary of Parameters Used in the PBPK-UGE Model

property (units)		values used in the model	literature values and source	descriptions
PBPK model	M_W(g·mol^{-1})	434.55	Chemspider	molecular weight
	LogP	2.2	2.2[21]	lipophilicity
	solubility (μg/mL)	51.2	51.2[9]	solubility in water
	P_{eff}(× 10^{-4} cm s^{-1})	4.8 (optimized)	27.5[21]	Caco-2 cell permeability
	f_{up}	0.038	3.8%[12]	fraction of free drug in plasma
	Rbp	0.58	calculated by PK-Sim	blood-to-plasma concentration ratio
	CL (L/h)	1.95 (optimized)	2.83[21]	total hepatic clearance
	CL_R(L/h)	GFR: 6.9 and 5.5		renal clearance
	GFR fraction	1.0		fraction of filtered drug in the urine
	partition coefficients	Rodgers and Rowland	optimized	calculation method from cell to plasma coefficients
	cellular permeabilities	PK-Sim standard	optimized	permeability calculation method across cell
UGE model	SGLT1 expression (μM)	0.049	6.8 pmol/mg protein[16]	concentration in the kidney for two cotransporters
	SGLT2 expression (μM)	0.19	18.4 pmol/mg protein[16]	
	ratio of IC_{50}	1770	1770[12]	ratio of LUS affinity to SGLT2 compared to SGLT1
	k_{on} for SGLT1 (μM^{-1}·h^{-1})	0.048 (calculated)		association rate constant
	k_{off} for SGLT1 (h^{-1})	0.11 (assumed)		
	k_{on} for SGLT2 (μM^{-1}·h^{-1})	84	1.4 × 10^{6}M^{-1}·min^{-1}[22]	dissociation rate constant
	k_{off} for SGLT2 (h^{-1})	0.11	1.8 × 10^{-3}min^{-1}[22]	
	$V_{max,S1,h}$(g/d)	89.4 (fitted)		maximum uptake velocity for healthy individuals and diabetes patients
	$V_{max,S2,h}$(g/d)	18.9 (calculated)		
	$V_{max,S1,T2DM}$(g/d)	119	119[24]	
	$V_{max,S2,T2DM}$(g/d)	25.2 (calculated)		
	K_m SGLT1 (mM)	1.8	1.8[15]	Michaelis−Menten constant for glucose to SGLT1/2
	K_m SGLT2 (mM)	4.9	4.9[15]	
	V_{plasma} (L)	2.5	default in PK-Sim	plasma volume
	$V_{lumen,S1}$ (L)	0.045	0.045[19]	S1 segment volume
	$V_{lumen,S2}$ (L)	0.019	0.019[19]	S2 segment volume
	$V_{bladder}$ (L)	0.2	0.2[19]	bladder volume
	Q_{lumen}(L/h)	2.7	2.7[19]	flow rate of the renal tubular lumen
	$Q_{bladder}$(L/h)	0.72	0.72[19]	flow rate of glucose excreted into the bladder
	Q_{urine}(L/h)	0.055	0.055[19]	flow rate of urine

distributions of LUS to the kidney in rats are wide, with kidney/plasma ratios of 6.0[11] and 35.3 at 4 h,[12] respectively. Unchanged LUS is to a lesser extent cleared through renal excretion, with approximately 5% recovered in the human urine.[9] Furthermore, previous studies have shown that LUS is only a weak inhibitor for CYP2C9 and a weak inducer for CYP3A4, with little effect on the other metabolizing enzymes and drug transporters.[13] LUS showed highly selective binding with SGLT2, with approximately 1770-fold higher affinity than to SGLT1 (mean IC_{50}: 2.26 nM versus 3990 nM) in in vitro experiments.[12]

In consideration of the significant contribution of SGLT2 to renal reabsorption of glucose along with the extremely high affinity to SGLT2 for LUS, it is anticipated that LUS can diminish RGR by approximately 90% when drug exposure is sufficient in the lumen of renal tubules. However, it was inconsistent with the clinical observations of the diabetics where only moderate inhibition in RGR was achieved after oral administration of LUS, even at a maximal clinical dose of 5 mg once daily. In a previous simulation study,[14] residual activities of SGLT2 and SGLT1 compensation have been put forward to analyze the differences between in vitro inhibition and in vivo observations. In a study,[15] it was found that there was no significant difference between the affinity for glucose to SGLT1 (K_m = 1.8 mM) and SGLT2 (K_m = 4.9 mM). Another paper[16] has shown that cotransporter expression in kidney tissue was also relatively close for SGLT1 (6.8 pmol/mg protein) and SGLT2 (18.4 pmol/mg protein). In view of the combination of affinity and protein expression, the two kidney cotransporters should have comparable potential in the RGR, or the contribution differences between them may not be as significant as previously perceived. To explain this, we set up a mathematical model to examine the factors causing this phenomenon.

Currently, only a few papers involving quantitative pharmacology modeling predicted the effects of several SGLT2 inhibitors on urine glucose excretion in humans.[14,17−20] Nevertheless, none of these papers involves quantitative simulation of LUS on UGE in humans using pharmacology modeling of PBPK combined SGLT2 occupancy (SO) and UGE models. Therefore, here, we developed a new mathematical model, termed as the PBPK-UGE model, where the PBPK model, SO model, and UGE model were incorporated. Next, under multiple dosage regimens, this model was utilized to (i) simulate the human PK profiles of LUS; (ii) simulate time-course profiles of SGLT2 occupancy by LUS; (iii) simulate the UGE rate-time profiles under multiple dosage regimens of LUS in humans; and (iv) analyze the underlying mechanism of moderate inhibition of RGR (23−40%) with the treatment of LUS, which is a highly potent inhibitor for SGLT2 (IC_{50} = 2.26 nM).

https://doi.org/10.1021/acsomega.2c06483
ACS Omega 2022, 7, 48427−48437

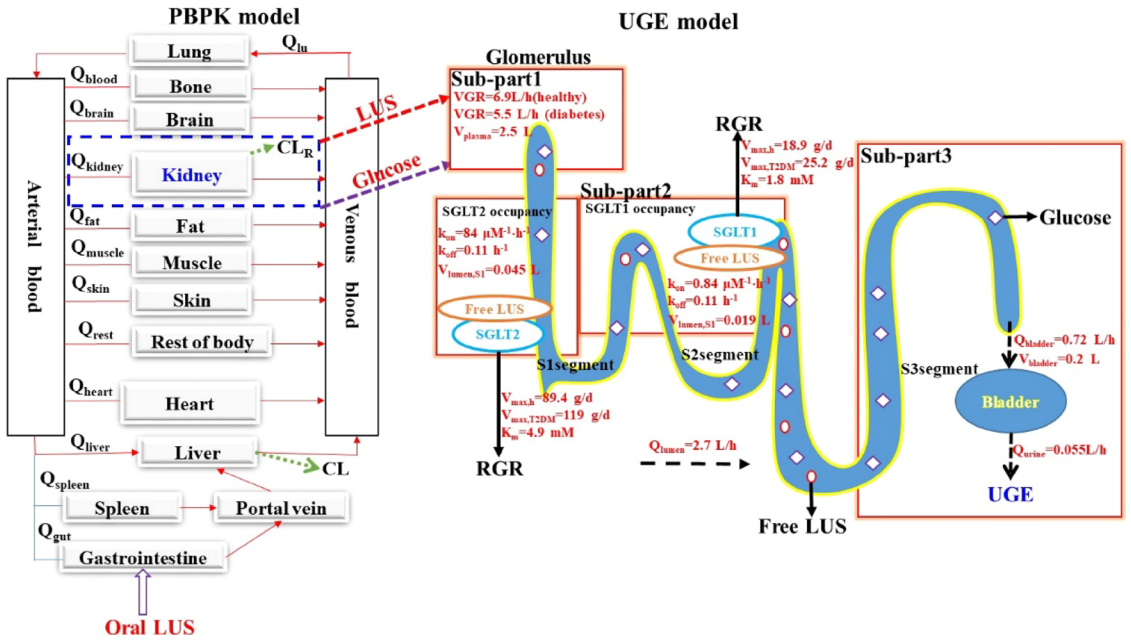

Figure 1. Structure of the PBPK-UGE model for LUS in humans. The model is composed of two parts. In the PBPK part, the C_{kt} of LUS can be predicted. In sub-part 1 of UGE, the free LUS concentration−time profiles in S1 and S2 segments can be simulated using C_{kt} combined eqs 1 and 2. In sub-part 2 of UGE, the time courses of the two cotransporter occupancies can be completely depicted using eqs 3−6. In sub-part 3 of UGE, the process of glucose transmission through renal tubules and the excretion through urine can be fully simulated using eqs 7−14.

2. MATERIALS AND METHODS

2.1. PBPK-UGE Model Development. *2.1.1. Software.* The PBPK-UGE model was constructed using PK-Sim and MoBi (Version 9.1, Bayer Technology Services, Leverkusen, Germany); Digit (Version 1.0.4, Simulations Plus, USA) was applied to digitize the figures of plasma concentration−time and UGE−time curves of LUS from the references; Origin 2019 (version 9.6.5.169, OriginLab, USA) was used to draw the figures. The V_{max} value was fitted using JMP (Version 11.0.0, SAS, USA).

2.1.2. Data Collection. A large number of literature studies were investigated to obtain the data for (i) model development: ① physicochemical and biochemical properties of LUS;[9,21] ② binding kinetics;[22] ③ affinity to SGLTs for glucose and expression of SGLT data;[15] and ④ physiological parameters for renal tubules.[19] The data have been summarized in Table 1. (ii) Model validation: ① PK validation: clinical PK concertation−time profiles[12,21,23,24] and ② UGE validation: clinical cumulative UGE−time and UGE rate−time profiles.[23,24]

2.1.3. Model Structure. The PBPK-UGE model is composed of two parts (PBPK model and UGE model). The PBPK model is connected by blood flow rate (Q) and tissue compartments, which involves the gastrointestine, blood (arterial supply and venous return), eliminating tissues (liver and kidney), and non-eliminating tissues (13 compartments in total, such as the lung).[25] The purpose of the PBPK model is to predict the LUS concentration in the kidney tissue (C_{kt}). C_{kt} can be predicted using C_{kt} (μM) = plasma concentration (μM) × $K_{p,Ki}$ (the renal partition coefficient of intracellular-to-plasma).

The renal tubules were separated into three compartments: the S1, S2, and S3 segments. SGLT2 and SGLT1 were expressed in the S1 and S2 segments, respectively. S3 is the bladder compartment. The division contributes to an accurate description of the change of luminal glucose concentration in the renal proximal tubule and the calculation of UGE over time. Since the three segments could achieve a good simulation between the observed and predicted UGE, the renal tubules were not divided into more sub-segments. Because the important contributors to RGR (SGLT1/2) are expressed in proximal tubules, the distal renal tubules are not incorporated into the present model owing to their irrelevance to RGR and UGE.[26] A bladder compartment is included in this model due to its relevance to the amount of UGE over time. The model structure and description are presented in Figure 1.

2.1.4. Model Parameters and Equations. The PBPK parameters in Table 1 were used to build the PBPK model, and the UGE parameters in Table 1 were used to develop the UGE model. The PBPK parameters were directly entered into PK-Sim to develop the PBPK model. The following eqs 12345678910111213 14 were used to build the UGE model. Most parameters in Table 1 were directly taken from the literature. More details for the optimized, assumed, and calculated parameters are as follows:

(i) Establishing the PBPK model: In the PK-Sim, the calculation of tissue distribution includes five methods: PK-Sim standard, Rodgers and Rowland, Schmitt, Poulin and Theil, and Berezhkovskiy, while the calculation of cellular permeability includes two methods: PK-Sim standard and charge-dependent Schmitt. However, the calculation of the disuse distribution for LUS has not been reported yet. As a result, the distribution calculation of LUS in the PBPK model was optimized by the module of parameter identification in the PK-Sim. The Rodgers and Rowland and PK-Sim standards were identified to calculate the tissue distribution and the cellular permeability, respectively. Based on previous studies on rats,[9,11,12] $K_{p,Ki}$ for LUS ranged from 6.0[9,11,12] to 35.3.[9,11,12] The data showed that the distribution of LUS in the kidney of rats was far higher compared with that in the plasma. To better match the observed PK profiles, the human $K_{p,Ki}$ was adjusted

https://doi.org/10.1021/acsomega.2c06483
ACS Omega 2022, 7, 48427−48437

to 12.0 in this simulation. The human effective permeability coefficient (P_{eff}) is typically correlated with the C_{max} of a drug. In this simulation, the P_{eff} ($\times 10^{-4}$ cm s^{-1}) of LUS was optimized at 4.8 from the reported data of 51.2 to make the predicted C_{max} close to the observed C_{max}. The P_{eff} values before and after the optimization showed that LUS is a high-permeability drug ($P_{eff} > 0.1 \times 10^{-4}$ cm s^{-1});[27] hence, it is considered a reasonable optimization within an acceptable range of parameters.

The elimination of LUS was assumed to be following hepatic clearance and renal excretion. To better match the predicted PK profiles with the observed PK profiles, the hepatic clearance of LUS (CL) was optimized to 1.95 L/h, while renal elimination was calculated by the product of GFR (glomerular filtration rate) and f_{up}. According to clinical data,[24] the GFR in T2DM patients was calculated at 5.5 L/h using the mean eGFR of the placebo group and four treatment groups, while the default GFR in healthy subjects in the PK-Sim is 115 mL/min (i.e., 6.9 L/h). Because it has not been reported that any renal kidney transporter or renal tubule could contribute to active secretion, reabsorption, and metabolism, fraction of GFR was hence set to 1.0. Additionally, it is worth pointing out that, except for GFR, the other corresponding physiological parameters from healthy humans were used when developing the PBPK model in patients with T2DM.

(ii) Establishing the UGE model: the development of sub-part 1. The following equations[19] were used to simulate free LUS concentration in S1 ($C_{LUS,S1}$) and S2 segments ($C_{LUS,S2}$) of renal tubules:

$$\frac{d(C_{LUS,S1})}{dt} = GFR \times C_{kt} \times f_{up} - Q_{lumen} \times \frac{C_{LUS,S1}}{V_{lumen,S1}} \quad (1)$$

$$\frac{d(C_{LUS,S2})}{dt} = Q_{lumen} \times \frac{C_{LUS,S1}}{V_{lumen,S1}} - Q_{bladder} \times \frac{C_{LUS,S2}}{V_{lumen,S2}} \quad (2)$$

f_{up} is the fraction of free LUS in plasma. Q_{lumen} denotes the physiological flux rate for proximal tubules. $V_{lumen,S1}$ is the volume of the S1 segment. $Q_{bladder}$ denotes the physiological flux rate for distal tubules. $V_{lumen,S2}$ is the volume of the S2 segment. The unit of C_{kt} is in μM.

In the development of sub-part 2 of the UGE model, the expression amount of SGLT1 and SGLT2 in the kidney was calculated to be 0.049 and 0.19 μM, respectively, by relative abundance (6.8 vs 18.4 pmol/mg microsomal protein)[16] $\times$ microsomal protein (26.2 mg/g kidney)[28] $\times$ kidney weight (about 273 g for a 62 kg person)[29] from the literature. In addition, the on-rate (k_{on}) and off-rate (k_{off}) of LUS toward SGLT1 have not been experimentally determined yet. The k_{off} of LUS from SGLT1 was hence set to the same value as that from SGLT2. The k_{on} of LUS on SGLT1 was set to 0.048 μM^{-1} h^{-1} referring to the in vitro IC_{50} ratio of SGLT1/SGLT2. The bindings of LUS to SGLT1/2 conform to the slow-binding mechanism, and these bindings are characterized by the combination of increased SGLT2 activity inhibition over time and no immediate recovery of SGLT2 activity when the inhibitor concentration approaches zero.[30] The residence time of LUS on SGLT2 is 9.1 h (residence time = $1/k_{off}$). In other words, LUS still engages SGLT2 for about 9.1 h after LUS is fully cleared in the human plasma. Hence, LUS can also be known as a time-dependent inhibitor of SGLT2. The inhibition processes of LUS to SGLT1 and SGLT2 can be better described by binding kinetics. The equations are as follows:

$$\frac{dLS_i}{dt} = k_{on,i} \times C_{lus,Si} \times S_{free,i} - k_{off,i} \times LS_i \quad (3)$$

$$\frac{dS_{free,i}}{dt} = -k_{on,i} \times C_{lus,Si} \times S_{free,i} + k_{off,i} \times LS_i \quad (4)$$

$$S_{total,i} = S_{free,i} + LS_i \quad (5)$$

$$TO_{SGLT,i} = \frac{LS_i}{S_{total,i}} \quad (6)$$

LS represents the concentration of the formed LUS−SGLT1/2 complex. S_{free} is the concentration of free SGLT1/2. S_{total} is the sum of LS and S_{free} (0.049 vs 0.19 μM for SGLT1 vs SGLT2). $TO_{SGLT,i}$ represents the fractional level of SGLT1/2 occupancy; i = 1 and 2 corresponds to SGLT1 and SGLT2, respectively.

In the development of sub-part 3 of the UGE model, the rate of glucose filtration from the plasma to renal tubules (RG_{plasma}) is given:

$$RG_{plasma} = C_{glu-plasma} \times GFR \quad (7)$$

The rate of glucose flux entering the bladder through renal tubules follows a first-order process, and glucose concentration in the S1 segment ($C_{glu,S1}$) is calculated as follows:[19]

$$\frac{dC_{glu,S1}}{dt} = RG_{plasma} - RRG_{S1} - Q_{lumen} \times \frac{C_{glu,S1}}{V_{lumen,S1}} \quad (8)$$

$C_{glu\text{-}plasma}$ is the glucose concentration in the plasma. The mean $C_{glu\text{-}plasma}$ before and after meals was set at 6.3 mM in healthy subjects and at 13.4 mM (0.5 mg), 11.8 mM (1 mg), 13.4 mM (2.5 mg), and 12.5 mM (5.0 mg) in T2DM patients according to clinical human data.[23,24] RRG_{S1} denotes the rate of renal glucose reabsorption in the S1 segment. To enable this simulation, the $C_{glu\text{-}plasma}$ data were taken from clinical data on healthy humans[23] and patients with T2DM[24] and then loaded into our model. The glucose concentration in the S2 segment ($C_{glu,S2}$) is calculated as follows:[19]

$$\frac{dC_{glu,S2}}{dt} = Q_{lumen} \times \frac{C_{glu,S1}}{V_{lumen,S1}} - RRG_{S2} - Q_{bladder} \times \frac{C_{glu,S2}}{V_{lumen,S2}} \quad (9)$$

RRG_{S2} denotes the rate of renal glucose reabsorption in the S2 segment. The initial rate of renal glucose reabsorption (RRG_0) is given using the following Michaelis−Menten equation in the absence of the inhibitor (at baseline):

$$RRG_0 = \frac{V_{max1,i} \times C_{glu,S1}}{K_{m,1} + C_{glu,S1}}(S1) + \frac{V_{max2,i} \times C_{glu,S2}}{K_{m,2} + C_{glu,S2}}(S2) \quad (10)$$

The following equations are used to calculate the rate of renal glucose reabsorption (RRG_i) in the presence of the inhibitor:

https://doi.org/10.1021/acsomega.2c06483
ACS Omega 2022, 7, 48427−48437

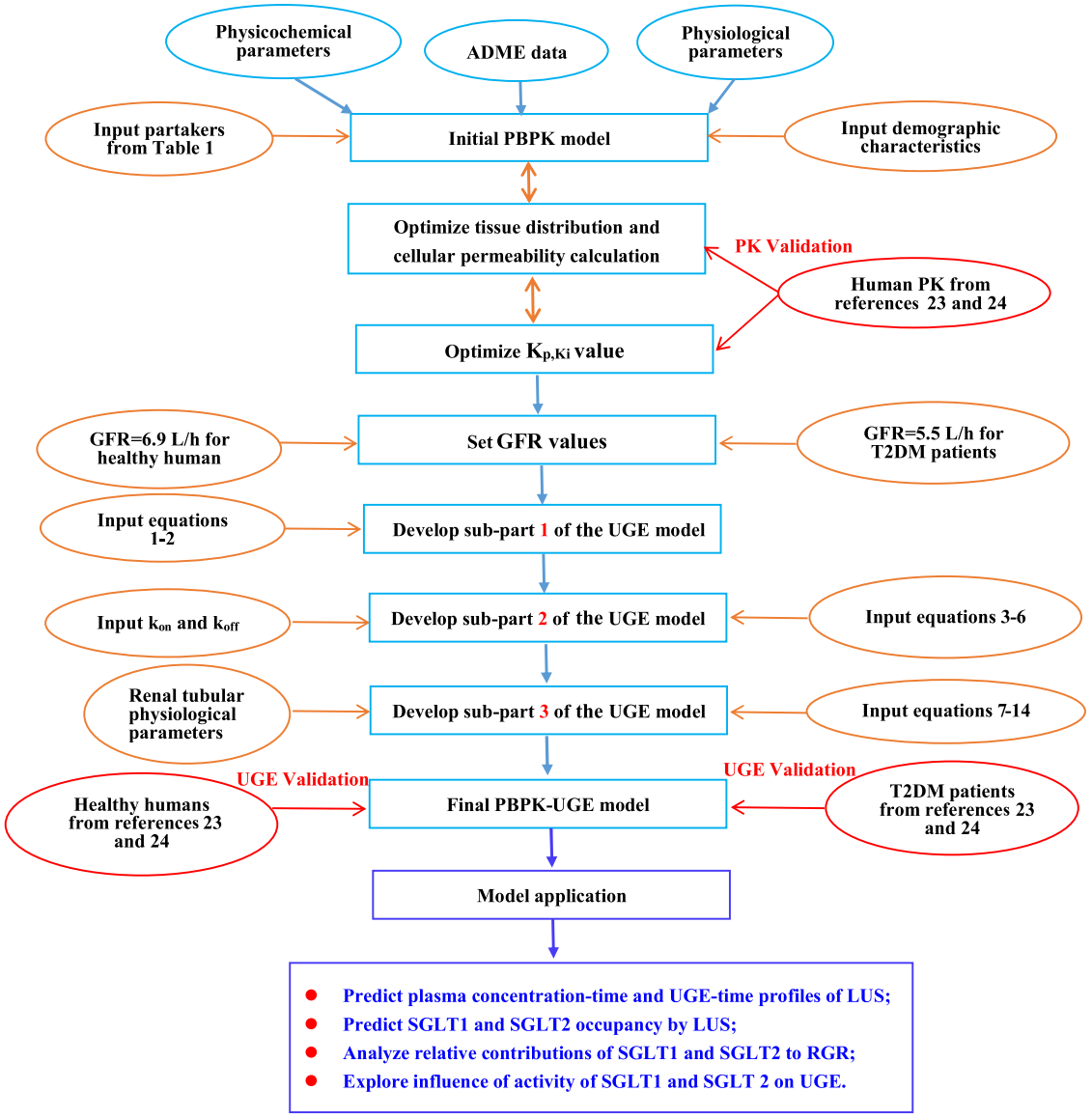

Figure 2. Workflow of LUS PBPK-UGE model development and validation. The model was built based on the parameters in Table 1, and some of parameters were optimized by comparing the predicted and observed PK data. Except for three parameters (plasma glucose concentration, GFR, and V_{max}), the model parameters in healthy individuals were the same as in T2DM patients. The models for healthy and T2DM subjects were both validated using the observed PK profiles (PBPK model validation) and UGE profiles (PBPK-UGE model validation) from the literature.[23,24]

$$\mathrm{RRG}_i = \frac{(1 - \mathrm{TO}_{\mathrm{SGLT1}}) \times V_{\mathrm{max1},i} \times C_{\mathrm{glu-lumen,S1}}}{K_{\mathrm{m},1} + C_{\mathrm{glu-lumen,S1}}}(\mathrm{S1}) + \frac{(1 - \mathrm{TO}_{\mathrm{SGLT2}}) \times V_{\mathrm{max2},i} \times C_{\mathrm{glu-lumen,S2}}}{K_{\mathrm{m},2} + C_{\mathrm{glu-lumen,S2}}}(\mathrm{S2}) \quad (11)$$

V_{max1} and V_{max2} represent the maximal rates of glucose reabsorption by SGLT2 and SGLT1, respectively. K_{m1} and K_{m2} denote glucose affinity constants for SGLT2 and SGLT1, respectively. $C_{glu,s1}$ and $C_{glu,s2}$ stand for glucose concentrations in S1 and S2 segments of renal tubules, respectively. V_{max} is fitted using the sigmoid maximal effect model as follows:[24]

$$\text{UGE amount of 24 h} = \frac{V_{\mathrm{max,sum}} \times \mathrm{AUC}^{\gamma}}{\mathrm{EC_{50}}^{\gamma} + \mathrm{AUC}^{\gamma}} \quad (12)$$

AUC represents the area under the PK curve at different doses. EC_{50} is the AUC at 50% of UGE. $V_{max,sum}$ is the sum (V_{max1} + V_{max2}) of the maximum rate of UGE. γ is the Hill coefficient. $V_{max,sum}$ is estimated using PK and UGE data of healthy humans without LUS and patients with T2DM after LUS administration,[23] respectively. In general, SGLT1 and SGLT2 are thought to be responsible for 10−20 and 80−90% reabsorption of renal glucose, respectively.[3,4] It was hence assumed that the V_{max1}/V_{max2} ratio was set at 5.7 (ratio mean 85% for SGLT2 over mean 15% for SGLT1) in this study. UGE is estimated using the following equation:[19]

$$\frac{\mathrm{dUGE}}{\mathrm{d}t} = Q_{\mathrm{urine}} \times \frac{C_{\mathrm{glu-bladder}}}{V_{\mathrm{bladder}}} \quad (13)$$

Q_{urine} is the flow rate of urine formation. $V_{bladder}$ is the bladder volume. When UGE−rate profiles were simulated, multiple glucose levels at different time points needed to be entered

https://doi.org/10.1021/acsomega.2c06483
ACS Omega 2022, 7, 48427−48437

into this model in turn. The glucose concentration in the urine ($C_{glu\text{-}bladder}$) is estimated by[19]

$$\frac{C_{glu-bladder}}{dt} = Q_{bladder} \times \frac{C_{glu-lumen,S2}}{V_{lumen,S2}} - Q_{urine} \times \frac{C_{glu-bladder}}{V_{bladder}} \quad (14)$$

2.2. PBPK-UGE Model Verification. The relevant PK and UGE profiles of healthy subjects and T2DM patients from the clinical studies[23,24] were used to validate the performance of the PBPK-UGE model. To verify this model, the figures of plasma concentration−time and UGE−time curves of LUS were first digitized with Digit software. Then, using this model, the PK and UGE profiles were quantitatively predicted in healthy humans and patients with T2DM after single ascending dose (SAD) for 1 day and after multiple ascending doses (MAD) for consecutive 7 days, respectively. Finally, the PK and UGE profiles simulated by the present model were compared with those observed in clinical studies.[23,24] The prediction performance of the model was evaluated by fold error of PK and UGE. The common acceptable value is within twofold of the parameters.[31] The workflow of LUS PBPK-UGE model development and validation is represented in Figure 2.

2.3. Simulations. *2.3.1. Virtual Demographic Characteristics.* Based on the demographic characteristics from these two clinical studies,[23,24] the PBPK-UGE model of LUS was built in eight virtual males, with a mean age of 26, mean weight of 61.5 kg, and BMI of 21.2 kg/m^2 for the healthy humans, and in eight virtual males, with a mean age of 58.8, mean weight of 66.8 kg, and BMI of 23.43 kg/m^2 for the patients with T2DM.

2.3.2. Occupancy Simulations toward SGLT1 and SGLT2. The SGLT1/2 occupancies by LUS were simulated by the PBPK-UGE model after oral administration of a single dose in healthy subjects and T2DM patients at 2.5 and 5 mg doses (clinical therapeutic dose), respectively. The glycemic concentration in healthy subjects and T2DM patients were set at 100 and 250 mg/dL, respectively.

2.3.3. Relative Contributions of SGLT1/2 to RGR. The RGRs by renal SGLT1 and SGLT2 were simulated in healthy individuals without LUS and after LUS treatment (2.5 and 5.0 mg). The mean glycemic concentration was set in the range of 100−300 mg/dL.

2.3.4. Influence of Reduced Activity of SGLT1/2 on Daily UGE. Owing to the genetic polymorphism of the population and different stages of T2DM, activity or expression of SGLT1/2 can be differentiated between different humans. Therefore, the simulations were carried out to examine the influence of reduced activity of SGLT1/2 on daily UGE in healthy individuals and T2DM patients without LUS and with LUS of 2.5 and 5 mg, respectively. The glycemic concentrations in healthy subjects and T2DM patients were set at 100 and 250 mg/dL, respectively. The V_{max} values used in the simulation for SGLT1 and SGLT2 were stepwise set at 20, 40, 60, 80, and 100% of their respective V_{max}.

3. RESULTS

3.1. Validation of PBPK-UGE Model Performance. As shown in Figure 3B, the predicted mean urinary excretion for 72 h was close to the observed value (5.4% vs 4.5%[9]). Overall, the PK simulations (Figure 3A,B) displayed that a satisfactory agreement between the predicted and clinically observed PK

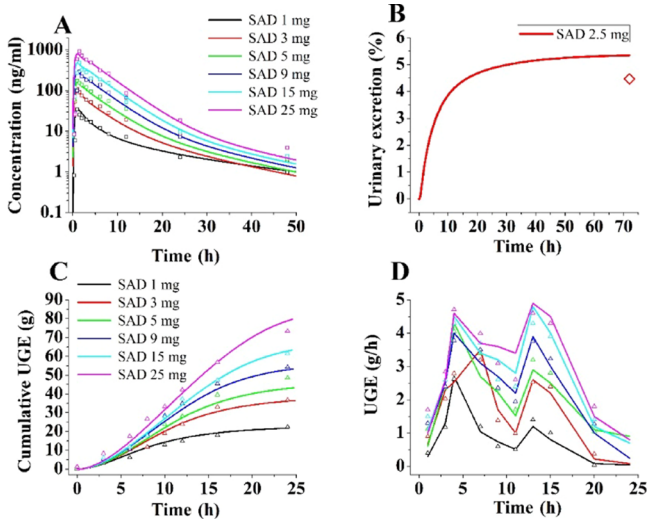

Figure 3. Simulations of pharmacokinetics and UGE of LUS in healthy subjects. Predicted and observed human plasma concentration−time curves of LUS after administration of SAD (A). Predicted and observed urinary excretion of LUS at a 2.5 mg dose (B). Cumulative UGE−time profiles (C) and UGE rate−time profiles (D) of LUS in healthy subjects after oral administration ranging from 1 mg to 25 mg. The squares (□) refer to observed oral pharmacokinetic data of LUS. The diamond (□) refers to cumulative urinary excretion of LUS in 72 h. The up triangles (△) refer to observed cumulative UGE (C) and UGE rate (D).

was achieved.[23] Figure 3C,D indicates a dose-dependent increase induced by LUS in cumulative UGE, which increased quickly at first and then slowed down, with a predicted 2.2-fold (observed 2.7-fold) from 1 to 5 mg dose, compared with a predicted 1.5-fold (observed 1.4-fold) from 5 to 25 mg dose for 24 h. On the whole, predicted UGE agreed well with the clinically determined data.[23]

Next, the PK and UGE of LUS were simulated following administration of MAD to further verify the predictive power of this model. A shown in Figure 4, the PBPK-UGE model can reproduce the observed PK profiles and cumulative UGE. The comparisons between predicted and observed data of LUS are given in Supplementary Tables S1−S3, where every fold error is within 2.0-fold.

On the whole, the present PBPK-UGE model can accurately predict PK profiles and fully describe cumulative and rate−time UGE data in healthy humans (where plasma glucose escalated from 89.1 to 167.0 mg/dL[23]) and patients (where plasma glucose escalated from 150.0 to 300.0 mg/dL[24]) with T2DM after LUS treatment.

3.2. Sensitivity Analysis of the Model. A sensitivity analysis was performed for cumulative daily UGE in T2DM patients at a 5 mg single dose of LUS with a mean plasma glucose range of 100−300 mg/dL. The simulations suggested that V_{max1} had a strong influence on daily UGE. The sensitivity of cumulative UGE to V_{max1} (at 4.1, 3.1, 2.1, and 1.0 mmol/h) is illustrated in Figure S1A. As expected, daily UGE gradually increased with the reduction of V_{max1}. Also, this increase largely depends on the plasma glucose concentration. A 50% decrease in V_{max2} (at 2.1 mmol/h) can result in urinary glucose ranging from 35% (300 mg/dL) to 97% (100 mg/dL). In addition, the sensitivity of daily UGE to K_{m2}, k_{on}, and k_{off} is depicted in Figure S1B,C,D. The simulations suggested that K_{m2} and k_{on}

https://doi.org/10.1021/acsomega.2c06483
ACS Omega 2022, 7, 48427−48437

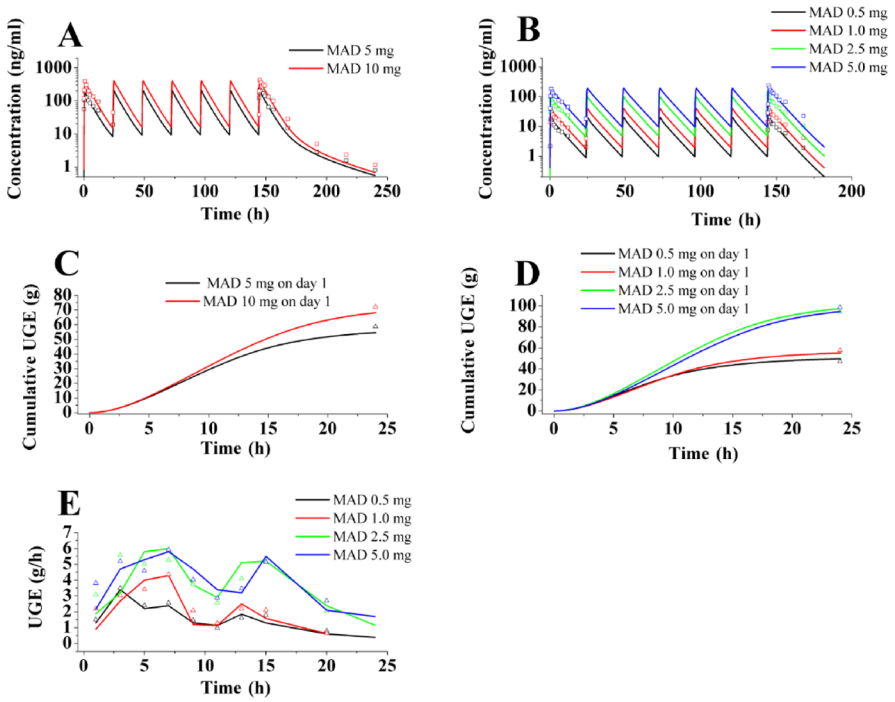

Figure 4. Human plasma concentration and UGE profiles of LUS following administration of MAD. Predicted and observed human plasma concentration−time curves of LUS in healthy subjects (A) and in T2DM patients (B) after administration of MAD. Cumulative UGE−time profiles in healthy subjects (C) and in T2DM patients (D), and UGE rate−time profiles in T2DM patients (E). The up-triangles (△) and squares (□) refer to observed clinical PK and UGE data of LUS, respectively.

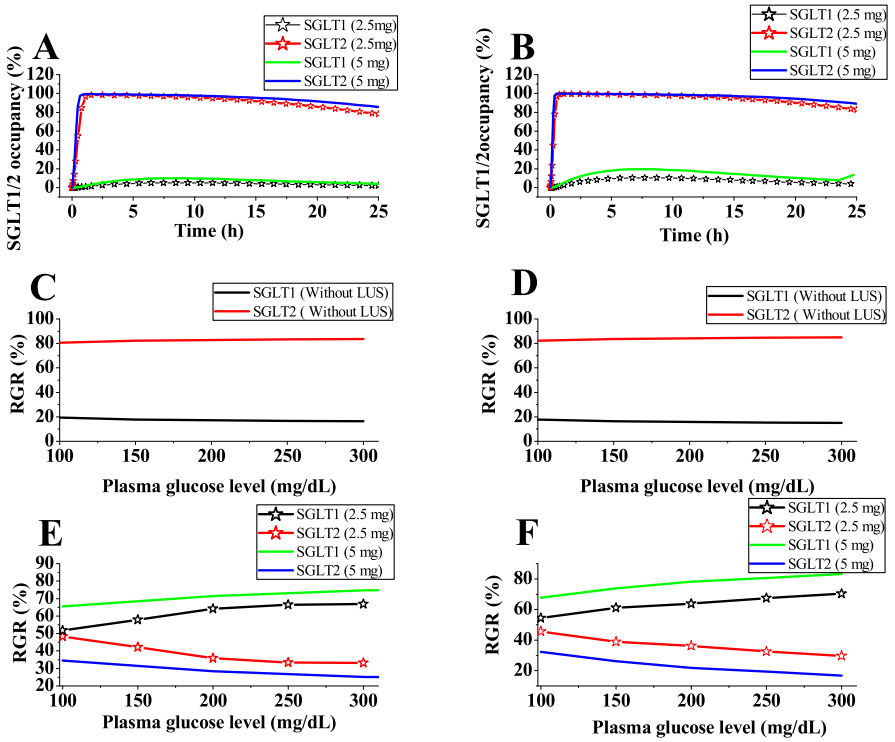

Figure 5. Calculated human SGLT2 occupancy time profiles by LUS (A) in healthy subjects and (B) in T2DM patients. The relative contributions to RGR by SGLT1/2 (C) in healthy subjects and in T2DM patients (D) without LUS and (E, F) with LUS.

had a mild and moderate influence on daily UGE, respectively, and UGE was insensitive to k_{off}.

3.3. Applications of the PBPK-UGE Model. *3.3.1. SGLT1 and SGLT2 Occupancy by LUS.* As shown in Figure 5A,B, in healthy individuals, the maximal occupancy (TO_{max}) for SGLT2 was 98.3% at 2.5 mg and 99.2% at 5 mg, while the duration of >90% SGLT2 occupancy ($D_{TO>90\%}$) was 16.3 and 20.7 h under the corresponding doses. In T2DM subjects, TO_{max} for SGLT2 was 99.3 and 99.6%, and $D_{TO>90\%}$ for SGLT2 was 19.9 and 24.1 h under the same doses. This

https://doi.org/10.1021/acsomega.2c06483
ACS Omega 2022, 7, 48427−48437

disparity mainly resulted from the smaller renal clearance in T2DM patients with a GFR of 5.5 L/h, compared to healthy subjects with a GFR of 6.9 L/h. Besides, the TO_{max} for SGLT1 was only 19.5 and 9.9% in healthy subjects and T2DM patients' simulations at 5 mg dose, respectively.

3.3.2. Relative Contributions to RGR between SGLT1 and SGLT2. As shown in Figure 5C,D, within a mean glycemic concentration of 100−300 mg/dL and in the absence of LUS, SGLT2 contributed approximately 85% of the total glucose reabsorption, while SGLT1 contributes about 15%. By contrast, in the presence of LUS, the contribution of SGLT2 declined and the contribution of SGLT1 to glucose reabsorption significantly increased (Figure 5E,F). With the LUS inhibition of 2.5 and 5 mg, SGLT1 contributed as much as approximately 52−76% of the total glucose reabsorption in healthy individuals (Figure 5E). Also, SGLT1 became the primary pathways of glucose reabsorption after LUS inhibition, contributing up to 70 and 83% of the total glucose reabsorption in T2DM patients.

3.3.3. Influence of Reduced Activity of SGLT1/2 on Daily UGE. In LUS treatment, SGLT1 activity had a massive influence on the UGE (Figure 6A). A 50% activity of SGLT1

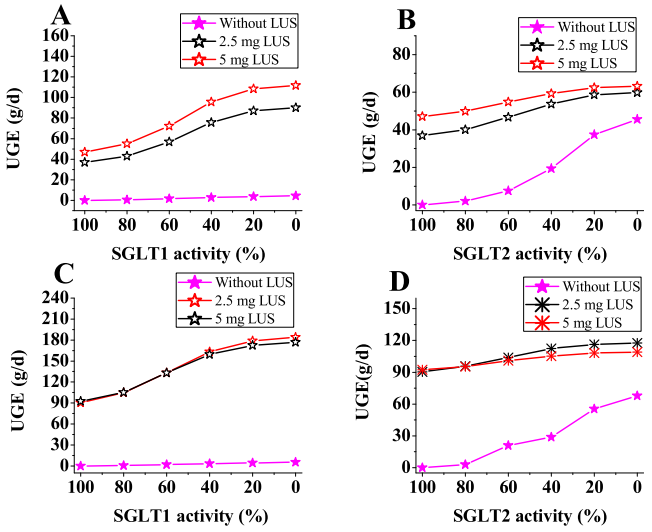

Figure 6. . Simulations of the influence of SGLT1/2 activity on the UGE in healthy subjects (A, B) and in T2DM patients (C, D).

caused a daily UGE of 70.6 (at 2.5 mg) and 87.1 g (at 5 mg). On the contrary, in the absence of LUS, as expected, SGLT2 activity had a significant effect on the UGE (Figure 6B). At a plasma glucose level of 118 mg/dL, 50% SGLT2 activity could result in a daily UGE of 18 g, while no SGLT2 activity could result in a daily UGE of 46 g. Similar results were also observed in the T2DM patients (Figure 6C,D).

4. DISCUSSION

The previous studies had proposed the hypotheses that the compensatory effect of SGLT1 played a key role in this seemingly discrepant observation between potent SGLT2 inhibition and moderate inhibition of RGR.[32,33] Also, the effect of SGLT1 compensation has been demonstrated in animals.[34] However, to date, the role of SGLT1 and SGLT2 in RGR in humans with or without inhibitors toward SGLT1/2 has not been experimentally confirmed yet, except for two simulation analyses.[14,19] Here, we used a new PBPK-UGE mathematical model of LUS to analyze the SGLT1 compensation effect as well as examine the influence of residual SGLT2 activity on RGR.

4.1. Characterization of SGLT1/2 RGR in the Absence of LUS. In this study, the ratios of V_{max1} and V_{max2} in healthy and T2DM subjects were both set at 4.7, which is quite close to the reported determined value in the rat (ratio of 5.4). Under near normoglycemic conditions (approximately 80−120 mg/dL) and without the treatment of LUS, SGLT1 and SGLT2 can exert about 69 and 96% of their respective V_{max} at peak glucose concentration in lumen S1 and S2 according to the Michaelis−Menten equation (eq 10). Nevertheless, owing to the sharp reduction in two luminal glucose levels to approach 0 at 3 h (Figure S2A), SGLT1 and SGLT2 can actually perform only a minor proportion of their V_{max}. With an increase in the plasma glucose level ranging from 100 to 300 mg/dL, at peak glucose concentration in lumen S1, the velocity of SGLT2 steadily increases to 90% of its maximal reaction velocity. Besides, SGLT1 and SGLT2 contribute to about 85 and 15% of the total RGR, respectively (Figure 5C,D).

4.2. Characterization of SGLT1/2 RGR in the Presence of LUS. From our simulation results, the maximal inhibition of SGLT2 could achieve nearly complete occupancy, and $DTO_{>90\%}$ for SGLT2 could last over 16 and 20 h (healthy and D2TM) at the clinical dosing regimen (2.5 and 5 mg once daily), respectively. Under multiple plasma glucose levels and with the treatment of LUS, the RGR activities of SGLT2 in healthy or T2DM subjects are all strongly inhibited, and residual SGLT2 activity is less than 10% for most of the time even after taking medicine at 5.0 mg. Consequently, the contribution of SGLT2 to RGR drops from about 85% without LUS treatment to 17−45% with LUS treatment.

When LUS is orally administered, the glucose concentration in the lumen of the renal tubules rises significantly and then declines steadily compared to that without LUS (Figure S2). Due to the prolonged high luminal glucose level (Figure S2E), the rate of RGR by SGLT1 is maintained at more than 90% for near 20 h. Moreover, the contribution of SGLT1 to RGR has been increasing and has reached approximately 83% with the increase in plasma glucose concentration. As a result, SGLT1 contributes to approximately 55−83% of total RGR when the majority of SGLT2 is occupied, which is about 3.7−5.5 times higher compared to about 15% of the contribution to RGR without LUS.

4.3. Theoretical Maximal Inhibition of RGR. The theoretical maximal inhibition of RGR by SGLT1/2 is illustrated in Figure S3. It was observed in this study that RGR is theoretically reduced to 52−67% (inhibition rate: 33−48%) when the activity of SGLT2 is completely suppressed (set V_{max} for SGLT2 as 0) (Figure S3A). Under a daily mean plasma glucose concentration of 150 mg/dL, total RGR is reduced to 63% with complete inhibition of SGLT2 (Figure S3A). On the other hand, when the SGLT1 completely loses its function (set V_{max} for SGLT1 as 0), it is observed that total RGR is theoretically reduced to about 18−34% (inhibition rate: 66−82%) at 5 mg of LUS (Figure S3A) and 85% without LUS (almost not affected by the increase in the plasma glucose level) in diabetic patients (Figure 5D), respectively. With a plasma glucose concentration of 150 mg/dL, total RGR is reduced to 28% with a complete loss in SGLT1 activity with 5 mg of LUS. The about 33% disparity (67% vs 34%) further supports the greater contribution of SGLT1 to total RGR with the treatment of LUS. In addition, the theoretical inhibition

https://doi.org/10.1021/acsomega.2c06483
ACS Omega 2022, 7, 48427−48437

range of RGR is 33−48% (V_{max} = 0 for SGLT2), wider than the inhibition range of RGR (23−40%) (Figure S3B), induced by SGLT2 inhibition with 5 mg of LUS. The approximately 10% disparity (33% vs 23%) corresponds to the contribution of unbound SGLT2 with LUS to total RGR.

Our simulation results are in good agreement with the findings in the mouse experiment, in which RGR in mice with knock-out of SGLT2 protein is reduced by about 50% of that in wild-type mice (33−48% reduction vs 50% reduction).[35] However, the predicted compensatory effect for SGLT1 by this simulation is not entirely consistent with the published experiment results (15% reduction in the simulation vs 3% reduction in mice).[36] As a whole, SGLT1 inhibition theoretically has only a slight effect on RGR (about 15% inhibition) without LUS and a strong effect with 5 mg of LUS (about 33−48% RGR reduction), while SGLT2 inhibition has a theoretically moderate effect on RGR (about 66−82% RGR reduction) with 5 mg of LUS.

4.4. Underlying Mechanism between High SGLT2 Occupancy and Moderate RGR Inhibition. At a maximal clinical dose of 5 mg, LUS strongly inhibits SGLT2 with near 100% occupancy and $D_{TO>90}$ as long as 24.1 h in T2DM patients. However, only moderate inhibition of RGR (23−40% inhibition) in the clinic was achieved. According to the current simulations as part of this study, it is possibly a combined result of the activity of unbound SGLT2 (not occupied) and SGLT1 compensatory effect. At clinical 5 mg LUS once daily, despite the very strong inhibition against SGLT2, it is not also likely to maintain 100% occupancy throughout the day. Therefore, more than 5% of SGLT2 is not occupied for nearly 6 h within an administration interval of 24 h. Consequently, a small amount of unbound SGLT2 retains the over 5% of the total reabsorption velocity. This residual activity induced by free SGLT2 roughly corresponds to 24% of the maximal reabsorption velocity induced by SGLT1 with a plasma glucose concentration of 150 mg/dL (5% × 119/25.2).

Meanwhile, when SGLT2 is almost completely occupied by LUS, lumen glucose concentration along the proximal tubules will remain high for a certain period of time, which can result in a sustained high reabsorption velocity for SGLT1. As a result, the increased reabsorption velocity of SGLT1 compensates for RGR reduction caused by SGLT2 inhibition. It has been demonstrated by the simulation results above in this study. With the increase in plasma glucose, the SGLT1 compensation effect also rises gradually; however, the contribution of residual activity of unbound SGLT2 on the inhibition of RGR is almost unchanged. Their ratios to SGLT1 and SGLT2 gradually change from 1:3 to 2.5. Although the contribution of unbound SGLT2 to the inhibition of RGR is relatively small under hyperglycemic conditions, the contribution of unbound SGLT2 should be taken into account as well under a mean plasma glucose of 100−300 mg/dL.

4.5. Inhibition of the SGLT1/2 Dual Inhibitor. Because the contribution of SGLT1 to RGR has significantly improved under the condition of SGLT2 occupancy, the SGLT1/2 dual inhibitor is theoretically beneficial to maximize UGE. However, sotagliflozin, a SGLT1/2 dual inhibitor with IC_{50} values of 1.8 nM for SGLT2 and 36 nM for SGLT1,[37] only induces small UGE with nearly 70 g/d at a clinical dose of 200 mg.[38] This probably is because of a lowered plasma glucose (only 180 mg/dL) induced by smaller glucose intake resulting from the inhibition of intestinal SGLT1 (both expressed in the small intestine and S2 segment of renal tubules). Another possible reason is that it is difficult for renal luminal inhibitor concentration to reach a sufficient level to suppress SGLT1 against the high renal luminal glucose competition. For example, with 5 mg of LUS and a plasma glucose concentration of 150 mg/dL, the glucose peak concentration in the S2 segment is about 60 nM, which is almost 33-fold of K_m for SGLT1. In order to outperform the competition against renal luminal glucose, luminal inhibitor concentration in the S2 segment must be at least 10-fold higher than the IC_{50}. However, because the peak level of LUS in the S2 segment is only 1.4 mM, it is less likely to be sufficient to inhibit SGLT1.

4.6. UGE Model Studies and Limitations. Several mathematical models for UGE have been published, including the UGE model in rat/mice,[39,40] UGE combined PK/PD model,[17,18] and system pharmacology model in humans.[14,19,20] Although this PBPK-UGE model has some advantages, we have also recognized that there are still some limitations to the present model. The biggest limitation is that it cannot simulate the dynamic change in the plasma glucose level induced by the combined result of glucose intake from food and regulation of glucose metabolism by insulin and UGE with LUS treatment. Therefore, during simulation, clinical observed mean plasma glucose concentration requires to be manually entered into this model. If the daily glycaemic-time profile could be predicted, it would further enhance the performance of this model. Another primary limitation is that the change in GFR in the establishment of the PBPK model for LUS in T2DM patients is only different from that in healthy subjects. The alterations of a more physiological factor in diabetes have not been taken into account in the present model yet. The third main limitation is that this model is currently only focused on the mean plasma glucose range of 100−300 mg/dL. Because of the lack of clinical UGE data for hyperglycemia, the prediction performance of this model has not been estimated yet above a mean plasma glucose level of 300 mg/dL.

5. CONCLUSIONS

In summary, the verified PBPK-UGE model has successfully predicted PK and UGE of LUS in healthy individuals and T2DM patients. The underlying mechanism has been explained using this model: a moderate inhibition of RGR with LUS (an SGLT2 strong inhibitor) is a result of the combined effect of two key factors, activity of unbound SGLT2 and the more important SGLT1 compensatory effect.

■ ASSOCIATED CONTENT

Supporting Information

The Supporting Information is available free of charge at https://pubs.acs.org/doi/10.1021/acsomega.2c06483.

(Supplementary Table S1) Observed and predicted PK for LUS according to the PBPK-UGE model in healthy subjects after SAD; (S2) observed and predicted PK for LUS according to the PBPK-UGE model in healthy and T2DM subjects after MAD; (S3) predicted and observed UGE of multiple doses according to the PBPK-UGE model; (Figure S1) sensitivity analysis; (Figure S2) simulations of free LUS concentration in the lumen of renal tubules with mean glucose concentration ranges of 100 mg/dL (A), 150 mg/dL (B), 200 mg/dL (C), 250 mg/dL (D), and 300 mg/dL (E); (Figure S3) theoretically maximal RGR inhibition rate (A) and calculated RGR inhibition rate using the model; (Figure

https://doi.org/10.1021/acsomega.2c06483
ACS Omega 2022, 7, 48427−48437

S4) predicted and observed human plasma concentration−time curves of LUS after administration of SAD; and (Figure S5) predicted and observed human plasma concentration−time curves of LUS in healthy subjects (A) and in T2DM patients (B) after administration of MAD (PDF)

AUTHOR INFORMATION

Corresponding Author

Jiawei Ren − *North China Electric Power University Hospital, Beijing 102206, China;* orcid.org/0000-0002-5701-4919; Phone: +86 18501256515; Email: rjw@ncepu.edu.cn

Authors

Zhongjian Wang − *Pharnexcloud Digital Technology Co., Ltd., Chengdu, Sichuan 610093, China*

Guopeng Wang − *Zhongcai Health (Beijing) Biological Technology Development Co., Ltd., Beijing 101500, China*

Complete contact information is available at: https://pubs.acs.org/10.1021/acsomega.2c06483

Author Contributions

‖Z.W. contributed equally to this work.

Funding

This research did not receive any specific grant from funding agencies in the public, commercial, or not-for-profit sectors.

Notes

The authors declare no competing financial interest.

REFERENCES

(1) Poulsen, S. B.; Fenton, R. A.; Rieg, T. Sodium-glucose cotransport. *Curr. Opin. Nephrol. Hypertens.* **2015**, *24*, 463−469.

(2) Wilcox, C. S. Antihypertensive and Renal Mechanisms of SGLT2 (Sodium-Glucose Linked Transporter 2) Inhibitors. *Hypertension* **2020**, *75*, 894−901.

(3) Sano, R.; Shinozaki, Y.; Ohta, T. Sodium-glucose cotransporters: Functional properties and pharmaceutical potential. *J. Diabetes Investig.* **2020**, *11*, 770−782.

(4) Defronzo, R. A.; Davidson, J. A.; Del Prato, S. The role of the kidneys in glucose homeostasis: a new path towards normalizing glycaemia. *Diabetes* **2012**, *14*, 5−14.

(5) Seino, Y. Luseogliflozin for the treatment of type 2 diabetes. *Expert Opin. Pharmacother.* **2014**, *15*, 2741−2749.

(6) Sakai, S.; Kaku, K.; Seino, Y.; Inagaki, N.; Haneda, M.; Sasaki, T.; Fukatsu, A.; Kakiuchi, H.; Samukawa, Y. Efficacy and Safety of the SGLT2 Inhibitor Luseogliflozin in Japanese Patients With Type 2 Diabetes Mellitus Stratified According to Baseline Body Mass Index: Pooled Analysis of Data From 52-Week Phase III Trials. *Clin. Ther.* **2016**, *38*, 843−862.e9.

(7) Markham, A.; Elkinson, S. Luseogliflozin: first global approval. *Drugs* **2014**, *74*, 945−950.

(8) Miyata, A.; Hasegawa, M.; Hachiuma, K.; Mori, H.; Horiuchi, N.; Mizuno-Yasuhira, A.; Chino, Y.; Jingu, S.; Sakai, S.; Samukawa, Y.; Nakai, Y.; Yamaguchi, J. Metabolite profiling and enzyme reaction phenotyping of luseogliflozin, a sodium-glucose cotransporter 2 inhibitor, in humans. *Xenobiotica* **2017**, *47*, 332−345.

(9) Pharmaceuticals and Medical Devices Agency (PMDA), https://www.info.pmda.go.jp/go/interview/1/400059_3969020F1020_1_014_1F.pdf.

(10) Samukawa, Y.; Sata, M.; Furihata, K.; Ito, T.; Ueda, N.; Ochiai, H.; Sakai, S.; Kumagai, Y. Luseogliflozin, an SGLT2 Inhibitor, in Japanese Patients With Mild/Moderate Hepatic Impairment: A Pharmacokinetic Study. *Clin. Pharmacol. Drug Dev.* **2017**, *6*, 439−447.

(11) Tahara, A.; Takasu, T.; Yokono, M.; Imamura, M.; Kurosaki, E. Characterization and comparison of sodium-glucose cotransporter 2 inhibitors in pharmacokinetics, pharmacodynamics, and pharmacologic effects. *J. Pharmacol. Sci.* **2016**, *130*, 159−169.

(12) Kakinuma, H.; Oi, T.; Hashimoto-Tsuchiya, Y.; Arai, M.; Kawakita, Y.; Fukasawa, Y.; Iida, I.; Hagima, N.; Takeuchi, H.; Chino, Y.; Asami, J.; Okumura-Kitajima, L.; Io, F.; Yamamoto, D.; Miyata, N.; Takahashi, T.; Uchida, S.; Yamamoto, K. (1S)-1,5-anhydro-1-[5-(4-ethoxybenzyl)-2-methoxy-4-methylphenyl]-1-thio-D-glucito l (TS-071) is a potent, selective sodium-dependent glucose cotransporter 2 (SGLT2) inhibitor for type 2 diabetes treatment. *J. Med. Chem.* **2010**, *53*, 3247−3261.

(13) Chino, Y.; Hasegawa, M.; Fukasawa, Y.; Mano, Y.; Bando, K.; Miyata, A.; Nakai, Y.; Endo, H.; Yamaguchi, J. I. In vitro evaluation of potential drug interactions mediated by cytochrome P450 and transporters for luseogliflozin, an SGLT2 inhibitor. *Xenobiotica* **2017**, *47*, 314−323.

(14) Lu, Y.; Griffen, S. C.; Boulton, D. W.; Leil, T. A. Use of systems pharmacology modeling to elucidate the operating characteristics of SGLT1 and SGLT2 in renal glucose reabsorption in humans. *Front. Pharmacol.* **2014**, *5*, 274.

(15) Hummel, C. S.; Lu, C.; Loo, D. D.; Hirayama, B. A.; Voss, A. A.; Wright, E. M. Glucose transport by human renal Na+/D-glucose cotransporters SGLT1 and SGLT2. *Am. J. Physiol.: Cell Physiol.* **2011**, *300*, C14−C21.

(16) Al-Majdoub, Z. M.; Scotcher, D.; Achour, B.; Barber, J.; Galetin, A.; Rostami-Hodjegan, A. Quantitative Proteomic Map of Enzymes and Transporters in the Human Kidney: Stepping Closer to Mechanistic Kidney Models to Define Local Kinetics. *Clin. Pharmacol. Ther.* **2021**, *110*, 1389−1400.

(17) Mori, K.; Saito, R.; Nakamaru, Y.; Shimizu, M.; Yamazaki, H. Physiologically based pharmacokinetic-pharmacodynamic modeling to predict concentrations and actions of sodium-dependent glucose transporter 2 inhibitor canagliflozin in human intestines and renal tubules. *Biopharm. Drug Dispos.* **2016**, *37*, 491−506.

(18) Samukawa, Y.; Mutoh, M.; Chen, S.; Mizui, N. Mechanism-based pharmacokinetic−pharmacodynamic modeling of luseogliflozin, a sodium glucose co-transporter 2 inhibitor, in Japanese patients with type 2 diabetes mellitus. *Biol. Pharm. Bull.* **2017**, *40*, 1207.

(19) Yakovleva, T.; Sokolov, V.; Chu, L.; Tang, W.; Greasley, P. J.; Peilot Sjögren, H.; Johansson, S.; Peskov, K.; Helmlinger, G.; Boulton, D. W.; Penland, R. C. Comparison of the urinary glucose excretion contributions of SGLT2 and SGLT1: A quantitative systems pharmacology analysis in healthy individuals and patients with type 2 diabetes treated with SGLT2 inhibitors. *Diabetes, Obes. Metab.* **2019**, *21*, 2684−2693.

(20) Mori-Anai, K.; Tashima, Y.; Nakada, T.; Nakamaru, Y.; Takahata, T.; Saito, R. Mechanistic evaluation of the effect of sodium-dependent glucose transporter 2 inhibitors on delayed glucose absorption in patients with type 2 diabetes mellitus using a quantitative systems pharmacology model of human systemic glucose dynamics. *Biopharm. Drug Dispos.* **2020**, *41*, 352−366.

(21) Mizuno-Yasuhira, A.; Nakai, Y.; Gunji, E.; Uchida, S.; Takahashi, T.; Kinoshita, K.; Jingu, S.; Sakai, S.; Samukawa, Y.; Yamaguchi, J. I. A Strategy for assessing potential drug-drug interactions of a concomitant agent against a drug absorbed via an intestinal transporter in humans. *Drug Metab. Dispos.* **2014**, *42*, 1456−1465.

(22) Uchida, S.; Mitani, A.; Gunji, E.; Takahashi, T.; Yamamoto, K. In vitro characterization of luseogliflozin, a potent and competitive sodium glucose co-transporter 2 inhibitor: Inhibition kinetics and binding studies. *J. Pharmacol. Sci.* **2015**, *128*, 54−57.

(23) Sasaki, T.; Seino, Y.; Fukatsu, A.; Sakai, S.; Samukawa, Y. Safety, pharmacokinetics, and pharmacodynamics of single and multiple luseogliflozin dosing in healthy Japanese males: a randomized, single-blind, placebo-controlled trial. *Adv. Ther.* **2014**, *31*, 345−361.

(24) Sasaki, T.; Seino, Y.; Fukatsu, A.; Ubukata, M.; Sakai, S.; Samukawa, Y. Pharmacokinetics, Pharmacodynamics, and Safety of

Luseogliflozin in Japanese Patients with Type 2 Diabetes Mellitus: A Randomized, Single-blind, Placebo-controlled Trial. *Adv. Ther.* **2015**, *32*, 319−340.
(25) Wang, Z.; Liu, W.; Li, X.; Chen, H.; Qi, D.; Pan, F.; Liu, H.; Yu, S.; Yi, B.; Wang, G.; Liu, Y. Physiologically based pharmacokinetic combined JAK2 occupancy modelling to simulate PK and PD of baricitinib with kidney transporter inhibitors and in patients with hepatic/renal impairment. *Regul. Toxicol. Pharmacol.* **2022**, *133*, No. 105210.
(26) Brown, E.; Rajeev, S. P.; Cuthbertson, D. J.; Wilding, J. P. A review of the mechanism of action, metabolic profile and haemodynamic effects of sodium-glucose co-transporter-2 inhibitors. *Diabetes Obes. Metab.* **2019**, *21*, 9−18.
(27) Alsenz, J.; Haenel, E. Development of a 7-day, 96-well Caco-2 permeability assay with high-throughput direct UV compound analysis. *Pharm. Res.* **2003**, *20*, 1961−1969.
(28) Scotcher, D.; Billington, S.; Brown, J.; Jones, C. R.; Brown, C. D.; Rostami-Hodjegan, A.; Galetin, A. Microsomal and Cytosolic Scaling Factors in Dog and Human Kidney Cortex and Application for In Vitro-In Vivo Extrapolation of Renal Metabolic Clearance. *Drug Metab. Dispos.* **2017**, *45*, 556−568.
(29) Brown, R. P.; Delp, M. D.; Lindstedt, S. L.; Rhomberg, L. R.; Beliles, R. P. Physiological parameter values for physiologically based pharmacokinetic models. *Toxicol. Ind. Health* **2016**, *13*, 407−484.
(30) Copeland, R. A.*Evaluation of Enzyme Inhibitors in Drug Discovery: A Guide for Medicinal Chemists and Pharmacologists, Second Edition*. Methods of biochemical analysis, 2005, vol *46*; pp 1−265.
(31) Li, G.; Yi, B.; Liu, J.; Jiang, X.; Pan, F.; Yang, W.; Liu, H.; Liu, Y.; Wang, G. Effect of CYP3A4 Inhibitors and Inducers on Pharmacokinetics and Pharmacodynamics of Saxagliptin and Active Metabolite M2 in Humans Using Physiological-Based Pharmacokinetic Combined DPP-4 Occupancy. *Front. Pharmacol.* **2021**, *12*, No. 746594.
(32) Liu, J. J.; Lee, T.; DeFronzo, R. A. Why Do SGLT2 inhibitors inhibit only 30-50% of renal glucose reabsorption in humans? *Diabetes* **2012**, *61*, 2199−2204.
(33) Abdul-Ghani, M. A.; DeFronzo, R. A.; Norton, L. Novel hypothesis to explain why SGLT2 inhibitors inhibit only 30-50% of filtered glucose load in humans. *Diabetes* **2013**, *62*, 3324−3328.
(34) Rieg, T.; Masuda, T.; Gerasimova, M.; Mayoux, E.; Platt, K.; Powell, D. R.; Thomson, S. C.; Koepsell, H.; Vallon, V. Increase in SGLT1-mediated transport explains renal glucose reabsorption during genetic and pharmacological SGLT2 inhibition in euglycemia. *Am. J. Physiol.: Renal Physiol.* **2014**, *306*, F188−F193.
(35) Vallon, V.; Platt, K. A.; Cunard, R.; Schroth, J.; Whaley, J.; Thomson, S. C.; Koepsell, H.; Rieg, T. SGLT2 mediates glucose reabsorption in the early proximal tubule. *J. Am. Soc. Nephrol.* **2011**, *22*, 104−112.
(36) Powell, D. R.; Dacosta, C. M.; Gay, J. Improved glycemic control in mice lacking Sglt1 and Sglt2. *Am. J. Physiol.: Endocrinol. Metab.* **2013**, *304*, E117−E130.
(37) Lapuerta, P.; Zambrowicz, B.; Strumph, P.; Sands, A. Development of sotagliflozin, a dual sodium-dependent glucose transporter 1/2 inhibitor. *Diab. Vasc. Dis. Res.* **2015**, *12*, 101−110.
(38) Rosenstock, J.; Cefalu, W. T.; Lapuerta, P.; Zambrowicz, B.; Ogbaa, I.; Banks, P.; Sands, A. Greater dose-ranging effects on A1C levels than on glucosuria with LX4211, a dual inhibitor of SGLT1 and SGLT2, in patients with type 2 diabetes on metformin monotherapy. *Diabetes Care* **2015**, *38*, 431−438.
(39) Yamaguchi, K.; Kato, M.; Suzuki, M.; Asanuma, K.; Aso, Y.; Ikeda, S.; Ishigai, M. Pharmacokinetic and pharmacodynamic modeling of the effect of an sodium-glucose cotransporter inhibitor, phlorizin, on renal glucose transport in rats. *Drug Metab. Dispos.* **2011**, *39*, 1801−1807.
(40) Yamaguchi, K.; Kato, M.; Ozawa, K.; Kawai, T.; Yata, T.; Aso, Y.; Ishigal, M.; Ikeda, S. Pharmacokinetic and pharmacodynamic modeling for the effect of sodium-glucose cotransporter inhibitors on blood glucose level and renal glucose excretion in db/db mice. *J. Pharm. Sci.* **2012**, *101*, 4347−4356.

https://doi.org/10.1021/acsomega.2c06483
ACS Omega 2022, 7, 48427−48437